J. Fluid Mech. (1990), *vol.* 218, *pp.* 531–546
Printed in Great Britain

Asymmetric Stokes flow between parallel planes due to a rotlet

By W. W. HACKBORN
Department of Mathematics, Camrose Lutheran College, Camrose, Alberta, Canada T4V 2R3

(Received 15 September 1988 and in revised form 11 July 1989)

An analysis is made of the Stokes flow between parallel planes due to a three-dimensional rotlet whose axis is parallel to the boundary planes. The separation in the plane of symmetry of this flow is compared with that in its two-dimensional analogue, the Stokes flow between parallel planes due to a two-dimensional rotlet. It is found that when the rotlets are midway between the planar walls, both flows exhibit an infinite set of Moffatt eddies. However, when the rotlets are not midway between the walls, the two-dimensional flow has an infinite set of Moffatt eddies, while the three-dimensional flow has at most a finite number of eddies and behaves, far from the rotlet, like the flow due to a two-dimensional source–sink doublet in each of the planes parallel to the boundary planes. An eigenfunction expansion describing a class of asymmetric Stokes flows between parallel planes is also derived and used to show that the far-field behaviour of flows in this class generally resembles the aforementioned flow due to a two-dimensional source–sink doublet in the planes parallel to the walls.

1. Introduction

In recent years, a number of studies have been made of Stokes flows in which flow separation and eddies may occur. In several of these studies, flows between parallel planar boundaries have been considered. For example, Moffatt (1964) considered an eigenfunction expansion for two-dimensional Stokes flow between parallel planes driven by an arbitrary disturbance and thereby discovered that such flows exhibit an infinite set of eddies. Liron & Mochon (1976) investigated the Stokes flow between parallel planes induced by a three-dimensional Stokeslet of arbitrary orientation. For the axisymmetric case in which the Stokeslet is normal to the planar walls, their analysis reveals (though it apparently was not noticed) that the flow contains an infinite set of eddies very similar to those of Moffatt; however, for the asymmetric case in which the Stokeslet is parallel to the walls, it was found that the flow far from the Stokeslet resembles that due to a two-dimensional source–sink doublet in each of the planes parallel to the walls. Another noteworthy example is that of Ganatos, Pfeffer & Weinbaum (1980) who used an analytical–numerical procedure to investigate the asymmetric Stokes flow between parallel planes induced by the translation or rotation of a sphere. Flow structure was only briefly examined in this study since a great deal of numerical work was required to accurately determine the velocity field; however, some flow separation was observed in the few cases considered. The flow examined in the present paper is essentially a special case of the flow due to a rotating sphere considered by Ganatos *et al.*

Some other studies have found the separation in a particular two-dimensional Stokes flow to be qualitatively the same as that in a plane of symmetry of the

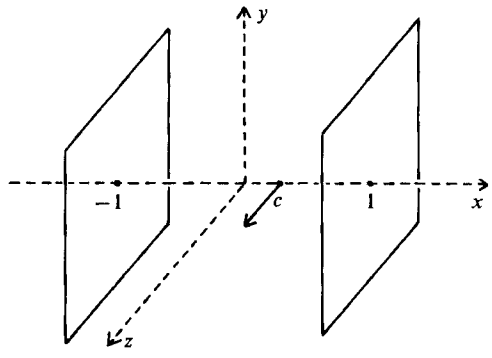

FIGURE 1. Geometry of the asymmetric flow. The direction of the torque induced by the rotlet is indicated by the solid arrow.

analogous three-dimensional flow. For example, Dorrepaal (1978, 1979) demonstrated the striking similarity between the separation in a two-dimensional streaming flow past a circular arc and that in a plane of symmetry of the three-dimensional (both axisymmetric and non-axisymmetric) streaming flow past a spherical cap. Another example is provided by Hackborn, O'Neill & Ranger (1986) who studied the Stokes flow inside a sphere due to a three-dimensional rotlet whose axis is perpendicular to a radius of the sphere; it was found that the separation in the plane of symmetry of this flow is qualitatively the same as that in the Stokes flow inside a circular cylinder due to a two-dimensional rotlet.

In this article, an analysis will be made of the asymmetric Stokes flow between parallel planes due to a three-dimensional rotlet whose axis is parallel to the boundary planes. The remarkable feature of this flow is the fact that the separation in its plane of symmetry generally differs radically from the separation in its two-dimensional analogue, the Stokes flow between parallel planes due to a two-dimensional rotlet. In particular, the two-dimensional flow always has an infinite set of Moffatt eddies; however, if the rotlet is not midway between the boundary planes, there is at most a finite number of eddies in the plane of symmetry of the three-dimensional flow, and the far-field behaviour of this flow, like that of the aforementioned asymmetric flow considered by Liron & Mochon, resembles the flow due to a two-dimensional source–sink doublet in the planes parallel to the boundaries.

The problem to be solved in determining the required asymmetric Stokes flow is stated in §2 and solved in §3. In §4, an asymptotic approximation to the flow far from the rotlet is found. The results of §§3 and 4 are used in §5 to describe some of the physical characteristics of the flow. In §6, the analogous two-dimensional flow is determined and compared to its three-dimensional analogue. Finally, an eigenfunction expansion for a class of asymmetric Stokes flows between parallel planes (similar to Moffatt's 1964 eigenfunction expansion for two-dimensional Stokes flows) is determined in §7 and used to draw some general conclusions about flows within that class.

2. Statement of the problem

The flow to be considered occurs between rigid parallel planes separated by a distance $2h$. The region between these planes is occupied by a homogeneous incompressible fluid of viscosity μ, and the motion of this fluid is generated by a three-dimensional rotlet (or point rotlet) of strength σ whose axis is parallel to the

boundary planes. By definition, a point rotlet is a singularity which exerts a torque of magnitude $8\pi\sigma\mu$ on the surrounding fluid, and the axis of the rotlet coincides with the direction of this torque. (A point rotlet can be regarded as a rotating sphere of infinitesimal radius.)

Assume that (x, y, z) are Cartesian coordinates considered to be dimensionless relative to h. Consequently, we may take the boundary planes to coincide with the planes $x = -1$ and $x = 1$. Furthermore, it is supposed that the rotlet lies at the point $(c, 0, 0)$, where $-1 < c < 1$, and that the torque induced by the rotlet is in the positive z-direction. The geometry of the flow is shown in figure 1. Note that the plane $z = 0$ is a plane of symmetry for the flow, and the plane $y = 0$ is a plane of antisymmetry.

Taking the fluid velocity $\boldsymbol{q}$ to be dimensionless relative to σ/h^2, the presence of the rotlet can be expressed by

$$\boldsymbol{q} = \boldsymbol{q}_0 + \boldsymbol{q}_1, \tag{2.1}$$

where $\boldsymbol{q}_0$, the velocity singularity representing the rotlet, is

$$\boldsymbol{q}_0 = \frac{\hat{\boldsymbol{k}} \times \boldsymbol{R}}{R^3}, \tag{2.2}$$

with $\boldsymbol{R} = (x-c)\,\hat{\boldsymbol{\imath}} + y\hat{\boldsymbol{\jmath}} + z\hat{\boldsymbol{k}}$, and $\boldsymbol{q}_1$ represents a Stokes flow with no singularities in the flow region $-1 < x < 1$. Assuming that the Reynolds number for the flow is zero, the flow is governed by the Stokes equation and the continuity equation, given respectively by

$$\nabla p = \nabla^2 \boldsymbol{q}, \quad \operatorname{div} \boldsymbol{q} = 0, \tag{2.3}$$

where p is the dimensionless pressure relative to $\mu\sigma/h^3$. Since the flow is not axisymmetric, it cannot be represented by only one scalar function. However, introducing cylindrical coordinates (x, ρ, ϕ) where $y = \rho\cos\phi$, $z = \rho\sin\phi$, $\rho \geqslant 0$, and $0 \leqslant \phi < 2\pi$, an appropriate representation for the solution to (2.3) using just two scalar functions is (from Ranger 1978)

$$\boldsymbol{q} = \operatorname{curl}\left[\operatorname{curl}\left(\frac{\psi}{\rho}\hat{\boldsymbol{\imath}}\cos\phi\right) + \frac{\chi}{\rho}\hat{\boldsymbol{\imath}}\sin\phi\right], \tag{2.4}$$

$$p = \frac{1}{\rho}\frac{\partial}{\partial x}(\mathrm{L}_{-1}\psi)\cos\phi, \tag{2.5}$$

where ψ and χ are scalar functions of x and ρ satisfying

$$\mathrm{L}_{-1}^2\psi = \mathrm{L}_{-1}\chi = 0, \tag{2.6}$$

and the operator L_{-1} is defined by

$$\mathrm{L}_{-1} \equiv \frac{\partial^2}{\partial x^2} + \frac{\partial^2}{\partial \rho^2} - \frac{1}{\rho}\frac{\partial}{\partial \rho}.$$

This flow representation is suitable when the boundaries consist of one or more finite or infinite coaxial circular discs.

From (2.4), the components of $\boldsymbol{q}$ in the directions of x, ρ and ϕ are respectively

$$q_x = -\frac{\partial}{\partial \rho}\left(\frac{1}{\rho}\frac{\partial \psi}{\partial \rho}\right)\cos\phi, \tag{2.7}$$

$$q_\rho = \left[\frac{\partial}{\partial \rho}\left(\frac{1}{\rho}\frac{\partial \psi}{\partial x}\right) + \frac{\chi}{\rho^2}\right]\cos\phi, \tag{2.8}$$

$$q_\phi = -\left[\frac{1}{\rho^2}\frac{\partial \psi}{\partial x} + \frac{\partial}{\partial \rho}\left(\frac{\chi}{\rho}\right)\right]\sin\phi. \tag{2.9}$$

Using equations (2.7)–(2.9), the no-slip boundary condition on the planes $x = -1$ and $x = 1$ may be expressed by

$$\frac{\partial}{\partial\rho}\left(\frac{1}{\rho}\frac{\partial\psi}{\partial\rho}\right) = 0, \quad x = \pm 1, \tag{2.10}$$

$$\frac{\partial}{\partial\rho}\left(\frac{1}{\rho}\frac{\partial\psi}{\partial x}\right)+\frac{\chi}{\rho^2} = 0, \quad x = \pm 1, \tag{2.11}$$

$$\frac{1}{\rho^2}\frac{\partial\psi}{\partial x}+\frac{\partial}{\partial\rho}\left(\frac{\chi}{\rho}\right) = 0, \quad x = \pm 1. \tag{2.12}$$

More useful boundary conditions can be obtained from (2.11) and (2.12) by eliminating either χ or $\partial\psi/\partial x$. Carrying this out yields

$$\frac{\partial}{\partial\rho}\left[\rho\frac{\partial}{\partial\rho}\left(\frac{1}{\rho}\frac{\partial\psi}{\partial x}\right)\right]-\frac{1}{\rho^2}\frac{\partial\psi}{\partial x} = 0, \quad x = \pm 1, \tag{2.13}$$

$$\frac{\partial}{\partial\rho}\left[\rho\frac{\partial}{\partial\rho}\left(\frac{\chi}{\rho}\right)\right]-\frac{\chi}{\rho^2} = 0, \quad x = \pm 1. \tag{2.14}$$

Finally, it must also be required that

$$\boldsymbol{q} \to 0 \quad \text{as} \quad \rho \to \infty. \tag{2.15}$$

3. Solution of the problem

From (2.2), the components of the velocity field $\boldsymbol{q}_0$ in the directions of x, ρ and ϕ are found to be

$$q_{0x} = -\rho R^{-3}\cos\phi, \quad q_{0\rho} = (x-c)R^{-3}\cos\phi, \quad q_{0\phi} = -(x-c)R^{-3}\sin\phi, \tag{3.1}$$

respectively, where $R = [(x-c)^2+\rho^2]^{\frac{1}{2}}$. Now, let ψ_0 and χ_0 be the scalar functions corresponding to $\boldsymbol{q}_0$ in accordance with (2.4). From (2.7)–(2.9) and the components of $\boldsymbol{q}_0$ in (3.1), solutions for ψ_0 and χ_0 are found to be

$$\psi_0 = -[(x-c)^2+\rho^2]^{\frac{1}{2}}, \quad \chi_0 = -(x-c)[(x-c)^2+\rho^2]^{-\frac{1}{2}}. \tag{3.2}$$

Representations for ψ and χ that satisfy (2.1) and (2.6) are

$$\psi = \psi_0+\int_0^\infty F(x,k)\,\rho J_1(k\rho)\,\mathrm{d}k, \quad \chi = \chi_0+\int_0^\infty G(x,k)\,\rho J_1(k\rho)\,\mathrm{d}k, \tag{3.3}$$

where J_1 is the Bessel function of the first kind of order 1, and

$$F(x,k) = A_1\cosh(kx)+A_2\sinh(kx)+A_3\,x\cosh(kx)+A_4\,x\sinh(kx), \tag{3.4}$$

$$G(x,k) = B_1\cosh(kx)+B_2\sinh(kx), \tag{3.5}$$

where A_1, A_2, A_3, A_4, B_1 and B_2 are functions of k.

Using (3.2), (3.3) and derivatives of Bessel functions given in Gradshteyn & Ryzhik (1965), boundary conditions (2.10), (2.13) and (2.14) may be expressed by

$$\int_0^\infty k^2F(\pm 1,k)\,J_1(k\rho)\,\mathrm{d}k = \rho[(c\mp 1)^2+\rho^2]^{-\frac{3}{2}}, \tag{3.6}$$

$$\int_0^\infty k^2F_x(\pm 1,k)\,J_1(k\rho)\,\mathrm{d}k = 3(c\mp 1)\rho[(c\mp 1)^2+\rho^2]^{-\frac{5}{2}}, \tag{3.7}$$

$$\int_0^\infty k^2G(\pm 1,k)\,J_1(k\rho)\,\mathrm{d}k = 3(c\mp 1)\rho[(c\mp 1)^2+\rho^2]^{-\frac{5}{2}}, \tag{3.8}$$

where F_x is the partial derivative of F with respect to x. Using the Hankel inversion theorem, (3.6)–(3.8) become

$$kF(\pm 1, k) = \int_0^\infty \rho^2[(c \mp 1)^2 + \rho^2]^{-\frac{3}{2}} J_1(k\rho)\,\mathrm{d}\rho, \tag{3.9}$$

$$kF_x(\pm 1, k) = kG(\pm 1, k) = 3(c \mp 1)\int_0^\infty \rho^2[(c \mp 1)^2 + \rho^2]^{-\frac{5}{2}} J_1(k\rho)\,\mathrm{d}\rho. \tag{3.10}$$

The integrals above can be evaluated using integration by parts and integrals provided in Gradshteyn & Ryzhik (1965), giving

$$kF(\pm 1, k) = \mathrm{e}^{-k(1 \mp c)}, \quad F_x(\pm 1, k) = G(\pm 1, k) = \mp\,\mathrm{e}^{-k(1 \mp c)}. \tag{3.11}$$

The six unknowns in (3.4) and (3.5) can now be determined from the six equations provided in (3.11). Hence,

$$F(x, k) = \frac{[k^{-1}(2k + 1 - \mathrm{e}^{-2k})\cosh(kx) - 2x\sinh(kx)]\cosh(kc)}{\sinh(2k) + 2k} + \frac{[k^{-1}(2k + 1 + \mathrm{e}^{-2k})\sinh(kx) - 2x\cosh(kx)]\sinh(kc)}{\sinh(2k) - 2k}, \tag{3.12}$$

$$G(x, k) = \frac{-\mathrm{e}^{-k}\sinh(kc)\cosh(kx)}{\cosh k} - \frac{\mathrm{e}^{-k}\cosh(kc)\sinh(kx)}{\sinh k}. \tag{3.13}$$

The required solutions for ψ and χ are now completely specified by (3.2), (3.3), (3.12) and (3.13).

Substituting these solutions for ψ and χ into (2.7)–(2.9), the velocity components are found to be

$$q_x = \tilde{q}_x \cos\phi, \quad q_\rho = \tilde{q}_\rho \cos\phi, \quad q_\phi = \tilde{q}_\phi \sin\phi, \tag{3.14}$$

where

$$\tilde{q}_x = -\rho[(x-c)^2 + \rho^2]^{-\frac{3}{2}} + \int_0^\infty k^2 F(x, k)\, J_1(k\rho)\,\mathrm{d}k, \tag{3.15}$$

$$\tilde{q}_\rho = (x-c)[(x-c)^2 + \rho^2]^{-\frac{3}{2}} + \int_0^\infty (kF_x(x, k)\, J_0(k\rho) + [G(x, k) - F_x(x, k)]\,\rho^{-1} J_1(k\rho))\,\mathrm{d}k, \tag{3.16}$$

$$\tilde{q}_\phi = -(x-c)[(x-c)^2 + \rho^2]^{-\frac{3}{2}} + \int_0^\infty (-kG(x, k)\, J_0(k\rho) + [G(x, k) - F_x(x, k)]\,\rho^{-1} J_1(k\rho))\,\mathrm{d}k. \tag{3.17}$$

4. Asymptotic analysis

Although the expressions given above for the velocity components may be used to compute the streamlines of the flow, the best way to study the overall flow structure qualitatively is to use asymptotic approximations to the velocity components far from the rotlet. In order to derive these approximations, we shall first find series expansions for ψ and χ.

n	λ_n	μ_n
1	4.212392+2.250729i	7.497676+2.768678i
2	10.71254+3.103149i	13.89996+3.352210i
3	17.07336+3.551087i	20.23852+3.716768i

TABLE 1. The first three values of λ_n and μ_n computed from (4.7) and (4.8)

From (3.2), (3.3) and integrals given in Gradshteyn & Ryzhik (1965), we obtain, for $\rho > 0$,

$$\psi = -|x-c| + \int_0^\infty H(k)\,\rho J_1(k\rho)\,\mathrm{d}k, \tag{4.1}$$

where $H(k) = F(x,k) - k^{-1}\,\mathrm{e}^{-k|x-c|}$, and

$$\chi = -\operatorname{sgn}(x-c) + \int_0^\infty I(k)\,\rho J_1(k\rho)\,\mathrm{d}k, \tag{4.2}$$

where $I(k) = G(x,k) + \operatorname{sgn}(x-c)\,\mathrm{e}^{-k|x-c|}$ and $\operatorname{sgn}(x-c) = \begin{cases} 1, & x \geqslant c \\ -1, & x < c \end{cases}$.

Using (3.12), we find

$$H(k) = \frac{[\cosh(kx) - \cosh[k(x-2s)] - 2k(x-s)\sinh(kx)]\cosh(kc)}{k(\sinh(2k)+2k)} + \frac{[\sinh(kx) + \sinh[k(x-2s)] - 2k(x-s)\cosh(kx)]\sinh(kc)}{k(\sinh(2k)-2k)}, \tag{4.3}$$

where $s = \operatorname{sgn}(x-c)$. Now, (4.1), (4.3) and integration by parts give

$$\psi = -\tfrac{1}{2}(cx^3 + x^2 - 3cx + 1) + \int_0^\infty H'(k)\,J_0(k\rho)\,\mathrm{d}k. \tag{4.4}$$

Using the identity

$$J_0(u) = \frac{2}{\pi}\int_1^\infty (t^2-1)^{-\frac{1}{2}}\sin(ut)\,\mathrm{d}t, \quad u > 0, \tag{4.5}$$

from Gradshteyn & Ryzhik (1965), the integral in (4.4) may be written, for $\rho > 0$, as

$$\int_0^\infty H'(k)\,J_0(k\rho)\,\mathrm{d}k = \frac{1}{\pi\mathrm{i}}\int_1^\infty (t^2-1)^{-\frac{1}{2}}\,\mathrm{d}t \int_{-\infty}^\infty H'(k)\,\mathrm{e}^{\mathrm{i}k\rho t}\,\mathrm{d}k. \tag{4.6}$$

Regarding k as a complex variable, it can be seen from (4.3) that all singularities of $H(k)$ in the half-plane $\operatorname{Im}(k) > 0$ are simple poles occurring at $k = \frac{1}{2}\mathrm{i}\lambda_n, \frac{1}{2}\mathrm{i}\bar{\lambda}_n, \frac{1}{2}\mathrm{i}\mu_n, \frac{1}{2}\mathrm{i}\bar{\mu}_n$, for $n = 1, 2, \ldots$, where λ_n and μ_n are the values in the first quadrant satisfying

$$\sin\lambda_n + \lambda_n = 0, \quad \sin\mu_n - \mu_n = 0, \tag{4.7}$$

and are ordered by increasing real part. Asymptotic approximations for λ_n and μ_n, from Buchwald (1964), are

$$\lambda_n \sim \alpha_n + \mathrm{i}\log 2\alpha_n, \quad \mu_n \sim \beta_n + \mathrm{i}\log 2\beta_n, \tag{4.8}$$

where $\alpha_n = \frac{1}{2}(4n-1)\,\pi$ and $\beta_n = \frac{1}{2}(4n+1)\,\pi$. The first three values of λ_n and μ_n, computed using Newton iteration to seven significant digits, are given in table 1. Now, it can be shown that the integral of $H'(k)\,\mathrm{e}^{\mathrm{i}k\rho t}$ over the semicircle at infinity in

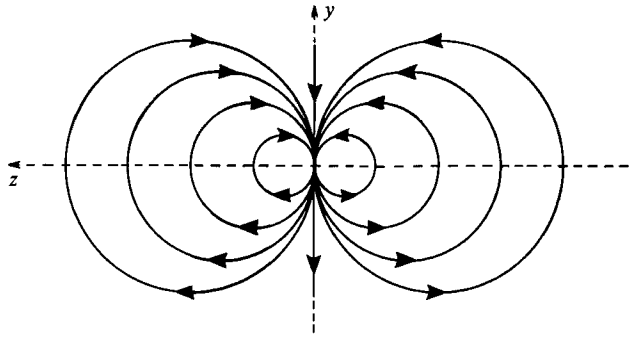

FIGURE 2. Streamlines of the far-field flow for $c \neq 0$ in a plane $x =$ constant. The flow directions shown are those for $c > 0$.

the half-plane $\mathrm{Im}\,(k) > 0$ vanishes when $\rho t > 0$; furthermore, the singularities of $H'(k)\,\mathrm{e}^{\mathrm{i}k\rho t}$ and $H(k)$ coincide. Thus, the integral of $H'(k)\,\mathrm{e}^{\mathrm{i}k\rho t}$ in (4.6) can be expressed in terms of its residues at $k = \frac{1}{2}\mathrm{i}\lambda_n, \frac{1}{2}\mathrm{i}\bar{\lambda}_n, \frac{1}{2}\mathrm{i}\mu_n, \frac{1}{2}\mathrm{i}\bar{\mu}_n$, for $n = 1, 2, \ldots$; carrying this out and using the identity

$$\int_1^\infty t(t^2-1)^{-\frac{1}{2}}\mathrm{e}^{-\alpha t}\,\mathrm{d}t = K_1(\alpha), \quad \mathrm{Re}\,(\alpha) > 0, \tag{4.9}$$

from Gradshteyn & Ryzhik (1965), where K_1 denotes the principal value of the modified Bessel function of the second kind of order 1, produces a series expansion for the integral on the left-hand side of (4.6). Combining this expansion with (4.4) gives

$$\psi = -\tfrac{1}{2}(cx^3+x^2-3cx+1) - 4\,\mathrm{Re}\sum_{n=1}^{\infty}[L_n(x)\,\rho K_1(\tfrac{1}{2}\lambda_n\rho) + M_n(x)\,\rho K_1(\tfrac{1}{2}\mu_n\rho)], \tag{4.10}$$

for $\rho > 0$, where

$$L_n(x) = \frac{[x\sin(\frac{1}{2}\lambda_n x) - \tan(\frac{1}{2}\lambda_n)\cos(\frac{1}{2}\lambda_n x)]\cos(\frac{1}{2}\lambda_n c)}{\cos\lambda_n + 1}, \tag{4.11}$$

$$M_n(x) = \frac{[x\cos(\frac{1}{2}\mu_n x) - \cot(\frac{1}{2}\mu_n)\sin(\frac{1}{2}\mu_n x)]\sin(\frac{1}{2}\mu_n c)}{\cos\mu_n - 1}. \tag{4.12}$$

If the steps that were applied to (4.1) to produce (4.10) are now applied to (4.2), we obtain, for $\rho > 0$,

$$\chi = -x + 2\sum_{n=1}^{\infty}[\sin((n-\tfrac{1}{2})\pi c)\cos((n-\tfrac{1}{2})\pi x)\,\rho K_1((n-\tfrac{1}{2})\pi\rho) - \cos(n\pi c)\sin(n\pi x)\,\rho K_1(n\pi\rho)]. \tag{4.13}$$

Equations (2.7)–(2.9) and the expansions for ψ and χ given in (4.10) and (4.13) can now be used to find expansions for the velocity components. For our purposes, it is sufficient to determine only the leading terms in these expansions. The asymptotic relation

$$K_1(u) \sim \left(\frac{\pi}{2u}\right)^{\frac{1}{2}}\mathrm{e}^{-u}[1+O(u^{-1})] \quad \text{as} \quad u \to \infty, \tag{4.14}$$

given in Gradshteyn & Ryzhik (1965), is used in the derivation of these terms.

c	0	0.001	0.01	0.1	0.25	0.5	0.75
ρ coords. of sep. pts.	1.017	1.018	1.027	1.126	ϕ	ϕ	0.7590
on $x=-1$, $\phi=0$	3.970	3.880	3.489	2.510	—	—	—
	6.777	—	—	—	—	—	—
	etc.	—	—	—	—	—	—
ρ coords. of sep. pts.	1.017	1.016	1.007	0.9185	0.7698	0.5098	0.2511
on $x=1$, $\phi=0$	3.970	4.105	—	—	—	—	—
	6.777	5.140	—	—	—	—	—
	etc.	—	—	—	—	—	—

TABLE 2. The ρ-coordinates of separation points on $x=\pm 1$, $\phi=0$ computed for several values of c

Surprisingly, the leading terms differ depending on whether or not $c=0$. When $c\neq 0$, it is found that

$$q_x \sim O(\rho^{-\frac{1}{2}}e^{-\frac{1}{2}\mathrm{Re}(\lambda_1)\rho}) \quad \text{as} \quad \rho\to\infty, \tag{4.15}$$

$$q_\rho \sim \tfrac{3}{2}c(x^2-1)\rho^{-2}\cos\phi + O(\rho^{-\frac{3}{2}}e^{-\frac{1}{2}\pi\rho}) \quad \text{as} \quad \rho\to\infty, \tag{4.16}$$

$$q_\phi \sim \tfrac{3}{2}c(x^2-1)\rho^{-2}\sin\phi + O(\rho^{-\frac{1}{2}}e^{-\frac{1}{2}\pi\rho}) \quad \text{as} \quad \rho\to\infty. \tag{4.17}$$

On the other hand, many terms in the expansions for the velocity components, including the leading terms in (4.16) and (4.17), vanish when $c=0$. Consequently, in this case,

$$q_x \sim \mathrm{Re}\,[\Lambda(x\sin(\tfrac{1}{2}\lambda_1 x)-\tan(\tfrac{1}{2}\lambda_1)\cos(\tfrac{1}{2}\lambda_1 x))\rho^{-\frac{1}{2}}e^{-\frac{1}{2}\lambda_1\rho}(1+O(\rho^{-1}))]\cos\phi + O(\rho^{-\frac{1}{2}}e^{-\frac{1}{2}\mathrm{Re}(\lambda_2)\rho}) \quad \text{as} \quad \rho\to\infty, \tag{4.18}$$

$$q_\rho \sim \mathrm{Re}\,[\Lambda(x\cos(\tfrac{1}{2}\lambda_1 x)-\cot(\tfrac{1}{2}\lambda_1)\sin(\tfrac{1}{2}\lambda_1 x))\rho^{-\frac{1}{2}}e^{-\frac{1}{2}\lambda_1\rho}(1+O(\rho^{-1}))]\cos\phi + O(\rho^{-\frac{3}{2}}e^{-\pi\rho}) \quad \text{as} \quad \rho\to\infty, \tag{4.19}$$

$$q_\phi \sim \mathrm{Re}\left[\frac{2\Lambda}{\lambda_1}(x\cos(\tfrac{1}{2}\lambda_1 x)-\cot(\tfrac{1}{2}\lambda_1)\sin(\tfrac{1}{2}\lambda_1 x))\rho^{-\frac{3}{2}}e^{-\frac{1}{2}\lambda_1\rho}(1+O(\rho^{-1}))\right]\sin\phi + O(\rho^{-\frac{1}{2}}e^{-\pi\rho}) \quad \text{as} \quad \rho\to\infty, \tag{4.20}$$

where $\Lambda=\pi^{\frac{1}{2}}\lambda_1^{\frac{3}{2}}/(1+\cos\lambda_1)$.

5. Flow description

For convenience, the components of the far-field velocity obtained by ignoring the $O(\ldots)$ terms in either (4.15)–(4.17), if $c\neq 0$, or (4.18)–(4.20), if $c=0$, will be denoted by q_x^*, q_ρ^* and q_ϕ^*, and the corresponding flow will be termed the far-field flow. We shall begin by examining the far-field flow.

First, the case $c\neq 0$ will be considered. Since $q_x^*=0$ in this case, the streamlines of the far-field flow lie in the planes $x=$ constant, for $-1<x<1$; hence, the far-field flow is two-dimensional in this sense. Now, consider the function

$$\Gamma = \tfrac{3}{2}c(1-x^2)\rho^{-1}\sin\phi. \tag{5.1}$$

Since $q_\rho^*=-\rho^{-1}\partial\Gamma/\partial\phi$ and $q_\phi^*=\partial\Gamma/\partial\rho$, it follows that Γ is a stream function for the two-dimensional flow occurring in a plane $x=$ constant. In fact, Γ represents the flow in an unbounded fluid due to a two-dimensional source–sink doublet of strength $\frac{3}{2}c(1-x^2)$, located at $\rho=0$ and oriented parallel to the y-axis. Hence, the streamlines of the far-field flow (i.e. the curves on which Γ and x are constant) are evidently circles in the planes $x=$ constant, and are tangent to the plane $z=0$ at $y=0$. (The

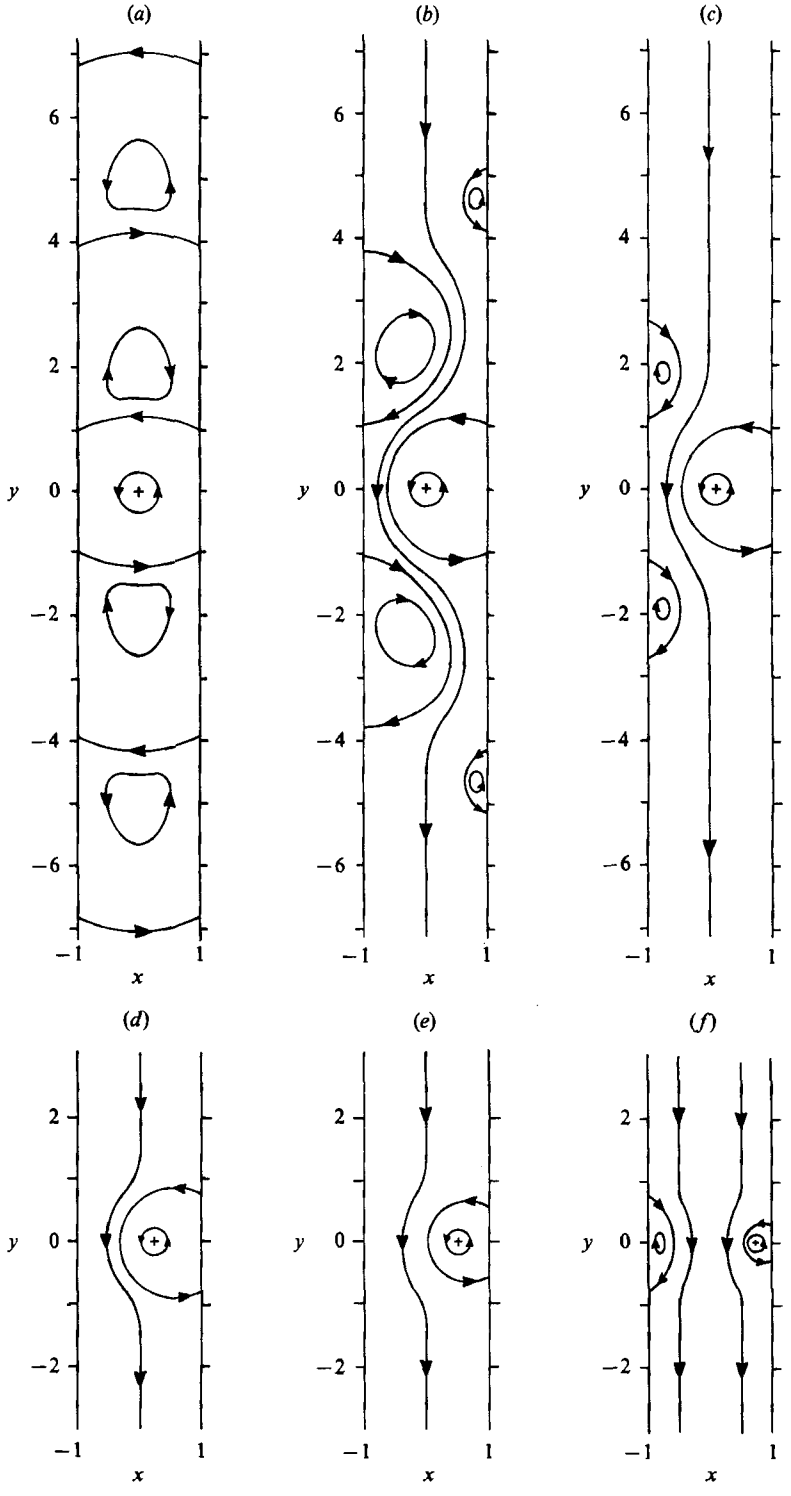

FIGURE 3. Schematic diagrams of streamlines in the plane $z = 0$ for (*a*) $c = 0$, (*b*) 0.001, (*c*) 0.1, (*d*) 0.25, (*e*) 0.5, and (*f*) 0.75. The position of the rotlet is indicated by +.

streamlines on which $z = 0$, $x =$ constant are regarded as circles of infinite radius.) Streamlines of the far-field flow for $c \neq 0$ in a plane $x =$ constant are shown in figure 2. Although the actual streamlines for $c \neq 0$ will differ somewhat from those depicted in figure 2, especially near the line $\rho = 0$, there are clearly closed streamlines comprising a large-scale recirculation on each side of the plane of symmetry $z = 0$ in the actual flow.

For the case $c = 0$, the far-field velocity components q_x^*, q_ρ^* and q_ϕ^*, given in (4.18)–(4.20), have the factor $\exp(-\frac{1}{2}\lambda_1 \rho)$. This indicates that the far-field flow consists of an infinite sequence of 'cells' of length (in the ρ-direction) $2\pi/\mathrm{Im}(\lambda_1) \approx 2.792$; the flow at corresponding points in adjacent cells (i.e. at points with the same x- and ϕ-coordinates but differing by $2\pi/\mathrm{Im}(\lambda_1)$ in the ρ-coordinate) differs in speed by a factor of about $\exp[\pi\,\mathrm{Re}(\lambda_1)/(\mathrm{Im}(\lambda_1)] \approx 358$ and is roughly in opposite directions.

The actual flow in the plane of symmetry $z = 0$ (or the azimuthal planes $\phi = 0$, $\phi = \pi$) will now be examined. When $c \neq 0$, the far-field flow determined above implies that streamlines in the plane $z = 0$ where ρ is sufficiently large are approximately straight lines on which x is constant; hence, eddies in the plane of symmetry $z = 0$ can exist only where ρ is sufficiently small. In contrast, when $c = 0$, the aforementioned sequence of cells in the far-field flow imply the existence of an infinite sequence of eddies in the plane $z = 0$ where ρ is sufficiently large.

The flow direction near a boundary is indicated by the vorticity (or, equivalently, the tangential stress) on that boundary. On the walls $x = \pm 1$ in the azimuthal plane $\phi = 0$, the vorticity curl $\boldsymbol{q} = \omega\hat{\boldsymbol{\phi}}$, where $\omega = \partial\tilde{q}_\rho/\partial x$. Flow separation points on $x = \pm 1$, $\phi = 0$ occur at ρ-values at which ω changes sign. The ρ-coordinates of separation points on $x = \pm 1$, $\phi = 0$ have been computed for several values of c using the expression for ω obtained by differentiating (3.16). These are provided, correct to four significant digits, in table 2. Note that separation points also occur on $x = \pm 1$, $\phi = \pi$ at the ρ-coordinates given in table 2.

Using the far-field flow and the boundary vorticity, schematic diagrams of streamlines in the plane of symmetry $z = 0$ can be drawn. Diagrams of this kind are given in figure 3 for various values of c. When $c = 0$, the flow exhibits an infinite sequence of eddies on each side of a 'separation region' (not considered to be an eddy) containing the rotlet, as depicted in figure 3(*a*). For small positive values of c, the flow in the plane $z = 0$ exhibits a finite number of eddies (in addition to the separation region containing the rotlet) attached alternately to the boundary planes $x = -1$ and $x = 1$. The remaining component of the flow in these cases consists of open streamlines which follow a circuitous path between the eddies. Figure 3(*b*) depicts a typical example of this kind of flow. As c increases from a small positive value, the number of eddies in the flow decreases rapidly until there are only two eddies (figure 3*c*) and eventually no eddies (figure 3*d*, *e*). As c continues to increase, a new eddy begins to grow on the wall $x = -1$ at $y = 0$ when $c \approx 0.65$, and this eddy continues to exist for all greater values of c less than 1 (figure 3*f*).

The flow in the plane of symmetry $z = 0$, as depicted in figure 3, contains some open streamlines when $c \neq 0$. These streamlines may suggest that there is a net volume flux between the boundary planes in the -y-direction when $c \neq 0$. This, of course, is not the case since the plane $z = 0$, having no thickness, can accommodate no volume flux; also, no net volume flux is associated with the flow in the region $z \neq 0$ since this flow consists entirely of closed streamlines.

It is worth noting that the flow behaviour shown in figure 3(*d*, *e*) is qualitatively identical to that induced by the rotating sphere between parallel planes depicted in

Ganatos *et al.* (1980). The flow description above is also partially confirmed by Blake & Chwang's (1974) solution for the flow beside a planar wall due to a point rotlet whose axis is parallel to the wall. Although Blake & Chwang did not look for separation in this flow, their solution implies a separation region like that attached to the boundary $x = 1$ in figure 3(f). Furthermore, the velocity decays at the same rate as that in the case $c \neq 0$ of the present study; however, as noted by Blake & Chwang, the streamlines far from a rotlet beside a single wall are approximately straight radial lines, and, therefore, these streamlines are open and are associated with a net volume flux.

6. Comparison with two-dimensional flow

The two-dimensional analogue of the three-dimensional flow examined above will now be briefly investigated. As before, the flow to be considered occurs between rigid parallel planes separated by a distance $2h$, and the fluid between these planes has viscosity μ. The flow is driven by a two-dimensional rotlet (or line rotlet) of strength σ. By definition, a line rotlet is a singularity which exerts a torque per unit length of magnitude $4\pi\sigma\mu$ on the surrounding fluid. (A line rotlet can be regarded as a rotating cylinder of infinitesimal radius.)

We again assume that the boundary planes coincide with the planes $x = -1$ and $x = 1$, where (x, y, z) are dimensionless Cartesian coordinates relative to h. The line rotlet is taken to coincide with the line $x = c$, $y = 0$, where $-1 < c < 1$. The flow is best represented using a stream function Ψ that is dimensionless relative to σ. If u and v are the components of the fluid velocity (assumed to be dimensionless relative to σ/h) in the x- and y-directions respectively, then

$$u = -\frac{\partial \Psi}{\partial y}, \quad v = \frac{\partial \Psi}{\partial x}. \tag{6.1}$$

The presence of the line rotlet may be expressed by

$$\Psi = \log R_1 + \tilde{\Psi}, \tag{6.2}$$

where $R_1 = [(x-c)^2 + y^2]^{\frac{1}{2}}$ and $\tilde{\Psi}$ represents a Stokes flow with no singularities in the flow region $-1 < x < 1$. The stream function for a Stokes flow is known to satisfy the biharmonic equation,

$$\nabla_1^4 \Psi = 0, \tag{6.3}$$

where ∇_1^2 is the two-dimensional Laplacian operator. From (6.1), the no-slip boundary condition on $x = \pm 1$ is seen to be satisfied if

$$\Psi = \frac{\partial \Psi}{\partial x} = 0, \quad x = \pm 1. \tag{6.4}$$

The solution of (6.2)–(6.4) for which $u \to 0$ and $v \to 0$ as $|y| \to \infty$ is readily found to be

$$\Psi = \tfrac{1}{2}\log\left(\frac{1 - 2\,\mathrm{e}^{\frac{1}{2}\pi y}\cos[\frac{1}{2}\pi(x-c)] + \mathrm{e}^{\pi y}}{1 + 2\,\mathrm{e}^{\frac{1}{2}\pi y}\cos[\frac{1}{2}\pi(x+c)] + \mathrm{e}^{\pi y}}\right) + \int_0^\infty h(x,k)\cos(ky)\,\mathrm{d}k, \tag{6.5}$$

where

$$h(x,k) = \frac{2[\tanh k\cosh(kx) - x\sinh(kx)]\cosh(kc)}{\sinh(2k) + 2k} + \frac{2[\coth k\sinh(kx) - x\cosh(kx)]\sinh(kc)}{\sinh(2k) - 2k}. \tag{6.6}$$

c	0	0.25	$c_1 \approx 0.4411$	0.5	0.75
y coords. of first two sep. pts.	1.024	0.8675	0	3.144	2.391
on $x = -1$	3.790	3.651	3.303	5.932	5.174
y coords. of first two sep. pts.	1.024	0.9059	0.6814	0.5995	0.2674
on $x = 1$	3.790	3.648	3.297	3.137	2.374

TABLE 3. The y-coordinates of the first two separation points in the region $y \geqslant 0$ on $x = \pm 1$ computed for several values of c

The first term in (6.5) is simply the stream function for the inviscid irrotational flow due to a line rotlet between parallel planes at $x = \pm 1$, and the second term is obtained using a Fourier transform. Details of the derivation of (6.5), (6.6) and other equations in this section are given in Hackborn (1987).

By expanding the first term in (6.5) using the Maclaurin series for $\log(1-\zeta)$ and expanding the second term using residue theory, it can be shown that

$$\Psi = 2\pi \operatorname{Re} \sum_{n=1}^{\infty} [L_n(x)\, e^{-\frac{1}{2}\lambda_n|y|} + M_n(x)\, e^{-\frac{1}{2}\mu_n|y|}], \tag{6.7}$$

for $y \neq 0$, where $L_n(x)$ and $M_n(x)$ are defined in (4.11) and (4.12), and λ_n and μ_n satisfy (4.7) and (4.8). From (6.1) and (6.7),

$$u \sim \operatorname{Re}[\tilde{A} \cos(\tfrac{1}{2}\lambda_1 c)(x \sin(\tfrac{1}{2}\lambda_1 x) - \tan(\tfrac{1}{2}\lambda_1) \cos(\tfrac{1}{2}\lambda_1 x))\, e^{-\frac{1}{2}\lambda_1|y|}] + O(e^{-\frac{1}{2}\operatorname{Re}(\mu_1)|y|}) \quad \text{as} \quad |y| \to \infty, \tag{6.8}$$

$$v \sim \operatorname{Re}[\tilde{A} \cos(\tfrac{1}{2}\lambda_1 c)(x \cos(\tfrac{1}{2}\lambda_1 x) - \cot(\tfrac{1}{2}\lambda_1) \sin(\tfrac{1}{2}\lambda_1 x))\, e^{-\frac{1}{2}\lambda_1|y|}] + O(e^{-\frac{1}{2}\operatorname{Re}(\mu_1)|y|}) \quad \text{as} \quad |y| \to \infty, \tag{6.9}$$

where $\tilde{A} = \pi\lambda_1/(1+\cos\lambda_1)$. Henceforth, the components of the far-field velocity obtained by ignoring the $O(\ldots)$ terms in (6.8) and (6.9) will be denoted by u^* and v^*, and the corresponding flow will be called the far-field flow. Now, the leading term of the expansion for Ψ given in (6.7) vanishes when

$$|y| = \frac{2}{\operatorname{Im}(\lambda_1)} (\arg[L_1(x)] + (m - \tfrac{1}{2})\pi), \tag{6.10}$$

where m takes integer values for which the right-hand side of (6.10) is positive when $-1 < x < 1$. Hence, the far-field flow consists of an infinite set of eddies which are separated by the curves described by (6.10) in the (x, y)-plane (or any other cross-sectional plane). Clearly, each eddy of the far-field flow has a length (in the y-direction) of $2\pi/\operatorname{Im}(\lambda_1) \approx 2.792$; moreover, owing to the presence of $\exp(-\frac{1}{2}\lambda_1|y|)$ in the expressions for u^* and v^*, the flow at corresponding points in adjacent eddies (i.e. at points with the same x-coordinate but differing by $2\pi/(\operatorname{Im}(\lambda_1)$ in the y-coordinate) differs in speed by a factor of $\exp[\pi \operatorname{Re}(\lambda_1)/\operatorname{Im}(\lambda_1)] \approx 358$ and is in opposite directions.

The preceding discussion of the far-field flow shows that the actual flow in the (x, y)-plane possesses infinitely many $\Psi = 0$ streamlines which are approximated increasingly well by (6.10) as $m \to \infty$ and which are the dividing streamlines of an infinite set of eddies. Flow separation points occur where the $\Psi = 0$ streamlines intersect the boundary planes $x = \pm 1$. These separation points can best be found by determining the y-values at which the scalar vorticity $\nabla_1^2 \Psi$ changes sign on $x = \pm 1$. The y-coordinates of the first two separation points in the region $y \geqslant 0$ on $x = \pm 1$

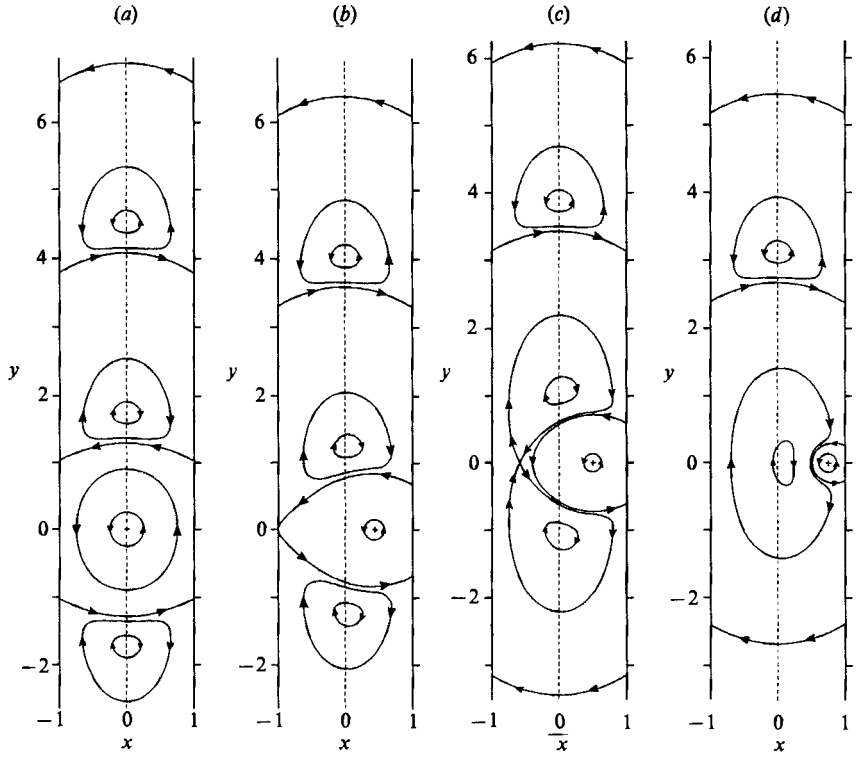

FIGURE 4. Accurate (computer-generated) plots of streamlines in the two-dimensional flow for (*a*) $c = 0$, (*b*) $c = c_1 \approx 0.4411$, (*c*) $c = 0.5$, and (*d*) $c = 0.75$. The position of the rotlet is indicated by +.

have been computed in this way and are provided, correct to four significant digits, in table 3 for several values of c. Note from table 3 that the y-coordinate of the first separation point on $x = -1$ decreases quickly until it equals 0 when $c = c_1$, where $c_1 \approx 0.4411$.

Some streamlines of the flow in the (x, y)-plane have been accurately plotted in figure 4 for several values of c. It is noteworthy that the flow has an unstable stagnation point on $y = 0$ for $c_1 < c < c_2$, where $c_2 \approx 0.6700$; this indicates that there is a 'figure-eight' pair of free eddies in the flow (as in figure 4*c*) for this range of c-values. It is also clear from figure 4 how quickly the flow converges to the far-field flow.

We can now compare the two-dimensional flow considered in this section with flow in the plane of symmetry of the three-dimensional flow considered previously. When $c = 0$, these two flows are evidently very similar. In this case, both flows exhibit an infinite set of eddies of roughly the same size, and the flow velocity in these eddies decays with distance from the rotlet at about the same exponential rate. In fact, the streamline patterns within the far-field eddies of the two flows are identical. (This follows from the fact that q_x^*/q_ρ^* and u^*/v^*, obtained from (4.18), (4.19), (6.8) and (6.9), have exactly the same form when $\phi = 0$ and $c = 0$ except for the constants A and $\tilde{A}$.) On the other hand, when $c \neq 0$, the two flows are radically different. In this case, for the three-dimensional flow, there is at most a finite number of eddies in the plane of symmetry and the velocity decays algebraically with distance from the rotlet; in contrast, for the two-dimensional flow, there continues to be infinitely many eddies and the velocity still decays exponentially.

It would appear that the large-scale recirculation in the three-dimensional flow when $c \neq 0$ (as depicted in figure 2) and the resulting open streamlines in the plane of symmetry cause the separation in this flow to differ so strikingly from that in its two-dimensional analogue. If a large-scale recirculation is precluded either by additional symmetry, as when $c = 0$, or by the boundary conditions, as in the asymmetric flow inside a sphere due to a point rotlet studied by Hackborn *et al.* (1986), then we expect the separation in the plane of symmetry of the three-dimensional flow to be similar to that in the analogous two-dimensional flow when recirculation is impossible.

A conjecture as to why the three-dimensional flow exhibits, when $c \neq 0$, a large-scale recirculation resembling the flow due to a two-dimensional source–sink doublet in the planes $x =$ constant may be that the separation points act like two-dimensional sources or sinks. In particular, the two separation points, one in the azimuthal plane $\phi = 0$ and the other in $\phi = \pi$ occurring at the smallest value of ρ seem to behave like a source–sink doublet in the following sense: fluid near the planar wall on which these separation points are located is pulled towards one of these points from all directions parallel to the wall; then, as it nears this point, the fluid is drawn away from the wall and eventually thrust back towards the wall near the other separation point from which it is pushed in all directions parallel to the wall. The combination of fluid being pulled towards one of these separation points while being pushed away from the other creates a source–sink doublet effect near the wall, and this effect possibly dominates the entire far-field flow since the velocity component normal to the walls is forced to decay exponentially.

7. General flow between parallel planes

Moffatt (1964) examined two-dimensional Stokes flow in a corner formed by two intersecting rigid planes. In the same paper, Moffatt briefly considered two-dimensional Stokes flow between parallel planes, which may be regarded as the limiting case of flow in a corner formed by two intersecting planes as the angle of the corner approaches 0. Letting (x, y, z) be dimensionless Cartesian coordinates as above, Moffatt showed that the dimensionless stream function Ψ for the flow between parallel planes at $x = \pm 1$ induced by an unspecified two-dimensional disturbance centred at $y = 0$ is

$$\Psi = \mathrm{Re} \sum_{n=1}^{\infty} [A_n(x \sin(\tfrac{1}{2}\lambda_n x) - \tan(\tfrac{1}{2}\lambda_n) \cos(\tfrac{1}{2}\lambda_n x)) \, \mathrm{e}^{-\frac{1}{2}\lambda_n |y|} + B_n(x \cos(\tfrac{1}{2}\mu_n x) - \cot(\tfrac{1}{2}\mu_n) \sin(\tfrac{1}{2}\mu_n x)) \, \mathrm{e}^{-\frac{1}{2}\mu_n |y|}], \quad (7.1)$$

for $y \neq 0$, where A_n and B_n are constants determined by the disturbance driving the flow, and λ_n and μ_n satisfy (4.7) and (4.8). (The expansion for Ψ in (7.1) is only implicit in Moffatt (1964); only the leading term is actually considered. To derive (7.1), one assumes that Ψ can be written as a series of separable solutions of (6.3) satisfying (6.4) for which the corresponding fluid velocity $\to 0$ as $|y| \to \infty$.) The expansion for Ψ given in (6.7), for the case in which the disturbance driving the flow is a line rotlet, is just a specific example of that given in (7.1), as one would expect. Moffatt was the first to discover that the leading term in (7.1) is associated with an infinite sequence of eddies on each side of the disturbance causing the flow. The eddies farthest from the rotlet in figure 4 are essentially 'Moffatt eddies'.

An analysis similar to that of Moffatt can also be done for a general asymmetric Stokes flow between rigid parallel planes for which the fluid velocity can be

represented by (2.4). Let (x, y, z) be dimensionless Cartesian coordinates and (x, ρ, ϕ) be the corresponding cylindrical coordinates, as defined in §2; assume further that ψ and χ are the scalar functions describing (in accordance with (2.4)) the dimensionless velocity $\boldsymbol{q}$ of a flow between parallel planes at $x = \pm 1$ induced by an unspecified disturbance centred at $\rho = 0$. It is readily seen that a separable solution for ψ in (2.6) has the form

$$\psi = \mathrm{Re}\,[f(x)\,\rho K_1(k\rho)],$$

for $\rho > 0$, where k is an eigenvalue to be determined and

$$f(x) = Ax\sin(kx) + Bx\cos(kx) + C\cos(kx) + D\sin(kx),$$

in which A, B, C and D are constants. Now, conditions (2.10) and (2.13) require that $f(x) = f'(x) = 0$ at $x \pm 1$. By considering separately the cases of an even $f(x)$ and an odd $f(x)$, we find that this requirement is satisfied by a non-trivial $f(x)$ if and only if $\sin(2k) \pm 2k = 0$. Owing to the asymptotic behaviour of $K_1(k\rho)$, as given by (4.14), we also need $\mathrm{Re}\,(k) > 0$ to satisfy (2.15). It follows from (4.7) that $k = \frac{1}{2}\lambda_n$, $\frac{1}{2}\bar{\lambda}_n$, $\frac{1}{2}\mu_n$ or $\frac{1}{2}\bar{\mu}_n$, for $n = 1, 2, \ldots$, and the corresponding eigenfunctions are

$$\psi_{\mathrm{e}}^{(n)} = \mathrm{Re}\,[A_n(x\sin(\tfrac{1}{2}\lambda_n x) - \tan(\tfrac{1}{2}\lambda_n)\cos(\tfrac{1}{2}\lambda_n x))\,\rho K_1(\tfrac{1}{2}\lambda_n \rho)], \tag{7.2}$$

$$\psi_{\mathrm{o}}^{(n)} = \mathrm{Re}\,[B_n(x\cos(\tfrac{1}{2}\mu_n x) - \cot(\tfrac{1}{2}\mu_n)\sin(\tfrac{1}{2}\mu_n x))\,\rho K_1(\tfrac{1}{2}\mu_n \rho)]. \tag{7.3}$$

A separable solution for χ in (2.6) has the form

$$\chi = \mathrm{Re}\,[g(x)\,\rho K_1(k\rho)],$$

for $\rho > 0$, where, as above, k is an eigenvalue to be determined and

$$g(x) = C\cos(kx) + D\sin(kx).$$

Condition (2.14) requires that $g(x) = 0$ at $x = \pm 1$. This requirement allows a non-trivial $g(x)$ if and only if $\cos k = 0$ (for an even $g(x)$) or $\sin k = 0$ (for an odd $g(x)$). Hence, $k = (n - \frac{1}{2})\pi$ or $k = n\pi$, for $n = 1, 2, \ldots$ (since we need $\mathrm{Re}\,(k) > 0$), and the corresponding eigenfunctions are

$$\chi_{\mathrm{e}}^{(n)} = C_n\cos((n-\tfrac{1}{2})\pi x)\,\rho K_1((n-\tfrac{1}{2})\pi\rho), \tag{7.4}$$

$$\chi_{\mathrm{o}}^{(n)} = D_n\sin(n\pi x)\,\rho K_1(n\pi\rho). \tag{7.5}$$

It is not difficult to show that the only other separable solutions of (2.6) for which the corresponding velocity is non-trivial and that satisfy (2.10)–(2.15) are

$$\psi^{(0)} = A_0 x^3 + B_0 x^2 + C_0 x + D_0, \quad \chi^{(0)} = 2B_0 x + 3A_0 + C_0, \tag{7.6}$$

for $\rho > 0$. Evidently, $\psi^{(0)}$ and $\chi^{(0)}$ are 'coupled' in the sense that their coefficients are related in order to satisfy (2.11) and (2.12). It is also noteworthy that the velocity corresponding to $\psi^{(0)}$ and $\chi^{(0)}$ is independent of B_0, C_0 and D_0.

Now, assuming that ψ and χ can be represented by series involving the separable solutions given in (7.2)–(7.6), we have

$$\psi = A_0 x^3 + B_0 x^2 + C_0 + D_0 + \mathrm{Re}\sum_{n=1}^{\infty}[A_n(x\sin(\tfrac{1}{2}\lambda_n x) - \tan(\tfrac{1}{2}\lambda_n)\cos(\tfrac{1}{2}\lambda_n x))\,\rho K_1(\tfrac{1}{2}\lambda_n\rho)$$
$$+ B_n(x\cos(\tfrac{1}{2}\mu_n x) - \cot(\tfrac{1}{2}\mu_n)\sin(\tfrac{1}{2}\mu_n x))\,\rho K_1(\tfrac{1}{2}\mu_n\rho)], \tag{7.7}$$

$$\chi = 2B_0 x + 3A_0 + C_0$$
$$+ \sum_{n=1}^{\infty}[C_n\cos((n-\tfrac{1}{2})\pi x)\,\rho K_1((n-\tfrac{1}{2})\pi\rho) + D_n\sin(n\pi x)\,\rho K_1(n\pi\rho)], \tag{7.8}$$

for $\rho > 0$, where the constants A_n, B_n, C_n and D_n ($n = 0, 1, 2, \ldots$) are determined by the disturbance driving the flow. The expansions for ψ and χ given in (4.10) and (4.13), for the case in which the disturbance is a point rotlet, are, of course, specific examples of those given in (7.7) and (7.8).

The result found above has considerable predictive value. To illustrate, consider a particular Stokes flow between parallel planes $x = \pm 1$ and for which the fluid velocity can be represented by (2.4). Without doing any calculations, we can assume that the functions ψ and χ describing this flow have the forms given in (7.7) and (7.8). Furthermore, provided that $A_0 \neq 0$, we can conclude that the velocity components for the flow are given by (4.15)–(4.17) (with $c = -2A_0$) and that the far-field flow is identical to the flow induced by a two-dimensional source–sink doublet (as depicted in figure 2) in each of the planes $x =$ constant. On the other hand, if the flow is antisymmetric about the plane $x = 0$ so that $A_0 = B_n = C_n = 0$ ($n = 1, 2, \ldots$) then, provided that $A_1 \neq 0$, the velocity components are given by (4.18)–(4.20) (with $A = -\frac{1}{4}\pi^{\frac{1}{2}}\lambda_1^{\frac{3}{2}}A_1$) and the far-field flow consists of an infinite sequence of cells. For example, if the disturbance driving the flow is a Stokeslet (point force) exerting a force $F\boldsymbol{j}$ at the point $(x, y, z) = (c, 0, 0)$, where $-1 < c < 1$, then the velocity can be represented by (2.4), and, since the flow is not antisymmetric about the plane $x = 0$, we expect that $A_0 \neq 0$. In fact, $A_0 = \frac{1}{2}(1-c^2)$ for this flow, taking $\boldsymbol{q}$ to be dimensionless relative to $F/(8\pi\mu h)$; this result was obtained from a study by Liron & Mochon (1976) of the Stokes flow between parallel planes due to a Stokeslet. As we would expect from the above remarks, Liron & Mochon found that, when the Stokeslet is parallel to the planar walls, the far-field flow is identical to the flow due to a two-dimensional source–sink doublet (with the same direction as the Stokeslet) in each of the planes parallel to the boundary planes.

REFERENCES

Blake, J. R. & Chwang, A. T. 1974 *J. Engng Maths* **8**, 23.

Buchwald, V. T. 1964 *Proc. R. Soc. Lond.* A **277**, 385.

Dorrepaal, J. M. 1978 *J. Engng Maths* **12**, 177.

Dorrepaal, J. M. 1979 *Z. Angew. Math. Phys.* **30**, 405.

Ganatos, P., Pfeffer, R. & Weinbaum, S. 1980 *J. Fluid Mech.* **99**, 755.

Gradshteyn, I. S. & Ryzhik, I. M. 1965 *Table of Integrals, Series, and Products.* Academic.

Hackborn, W. W. 1987 Separation in interior Stokes flows driven by rotlets. Ph.D. thesis, University of Toronto.

Hackborn, W. W., O'Neill, M. E. & Ranger, K. B. 1986 *Q. J. Mech. Appl. Maths* **39**, 1.

Liron, N. & Mochon, S. 1976 *J. Engng Maths* **10**, 287.

Moffatt, H. K. 1964 *J. Fluid Mech.* **18**, 1.

Ranger, K. B. 1978 *Intl J. Multiphase Flow* **4**, 263.